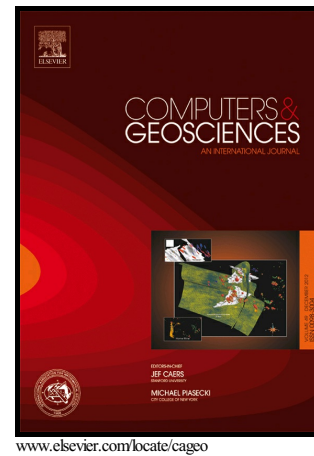


Author's Accepted Manuscript

spMC: an R-package for 3D lithological reconstructions based on spatial Markov chains

Luca Sartore, Paolo Fabbri, Carlo Gaetan



PII: S0098-3004(16)30147-9
DOI: <http://dx.doi.org/10.1016/j.cageo.2016.06.001>
Reference: CAGEO3771

To appear in: *Computers and Geosciences*

Received date: 8 October 2015
Revised date: 17 March 2016
Accepted date: 2 June 2016

Cite this article as: Luca Sartore, Paolo Fabbri and Carlo Gaetan, spMC: an R package for 3D lithological reconstructions based on spatial Markov chains *Computers and Geosciences*, <http://dx.doi.org/10.1016/j.cageo.2016.06.001>

This is a PDF file of an unedited manuscript that has been accepted for publication. As a service to our customers we are providing this early version of the manuscript. The manuscript will undergo copyediting, typesetting, and review of the resulting galley proof before it is published in its final citable form. Please note that during the production process errors may be discovered which could affect the content, and all legal disclaimers that apply to the journal pertain.

spMC: an R-package for 3D lithological reconstructions based on spatial Markov chains

Luca Sartore^{a,b}, Paolo Fabbri^c, Carlo Gaetan^b

^a*National Institute of Statistical Science, 19 T.W. Alexander Drive, P.O. Box 14006,
Research Triangle Park, NC 27709-4006, U.S.A.*

^b*Dipartimento di Scienze Ambientali, Informatica e Statistica, Università “Ca’ Foscari”
di Venezia, Campus Scientifico, Via Torino 155, I-30172 Mestre-Venezia, Italy*

^c*Dipartimento di Geoscienze, Università di Padova, via Gradenigo 6, 35131 Padova,
Italy*

Abstract

The paper presents the spatial Markov Chains (spMC) R-package and a case study of subsoil simulation/prediction located in a plain site of Northeastern Italy. spMC is a quite complete collection of advanced methods for data inspection, besides spMC implements Markov Chain models to estimate experimental transition probabilities of categorical lithological data. Furthermore, simulation methods based on most known prediction methods (as indicator Kriging and CoKriging) were implemented in spMC package. Moreover, other more advanced methods are available for simulations, e.g. path methods and Bayesian procedures, that exploit the maximum entropy. Since the spMC package was developed for intensive geostatistical computations, part of the code is implemented for parallel computations via the OpenMP constructs. A final analysis of this computational efficiency compares the simulation/prediction algorithms by using different numbers of CPU cores, and

Email addresses: lsartore@niss.org (Luca Sartore), paolo.fabbri@unipd.it (Paolo Fabbri), gaetan@unive.it (Carlo Gaetan)

considering the example data set of the case study included in the package.

Keywords: Categorical data, Transition probabilities, Transiogram modeling, Indicator CoKriging, Bayesian entropy, 3D lithological conditional simulation/prediction

1 **1. Introduction**

2 The paper aims to introduce the spMC package (Sartore, 2013) which
3 is an extension package for the R software (R Core Team, 2016). Its main
4 purpose is to provide recent tools for the analysis, simulation and predic-
5 tion of lithological data under the methodological framework of the spatial
6 Markov chains. The first software implementation of lithological simulation
7 and prediction for spatial Markov chains, stemming from the seminal work
8 of Carle and Fogg (1996, 1997), Carle et al. (1998), Weissmann et al. (1999),
9 and Weissmann and Fogg (1999), was the geostatistical software T-PROGS
10 (Carle, 1999). This software is a well-established stochastic modelling tool for
11 3-D applications and also embedded in some commercial groundwater mod-
12 elling software (e.g. GMS, Aquaveo, 2015). In T-PROGS transition proba-
13 bilities are estimated for describing the stratigraphical characteristics of the
14 geological data. Then simulations are performed through CoKriging and
15 simulated annealing methods. The spMC package in its present version is
16 a complete collection of advanced methods for data inspection, statistical
17 estimation of parameter models, and lithological simulation and prediction.
18 It includes common tools for predicting and simulating lithofacies at pixel
19 level which are typically used like sequential indicator simulation (SISIM,
20 Deutsch and Journel, 1998) as well as the more recent advances (Li, 2007;

21 Allard et al., 2011). We think there are three features of spMC that can be
 22 of value in the geostatistical community. First, it is an extension package
 23 of an increasingly used software like R. Second, a particular strength of the
 24 package is the exploitation of high performance computational (HPC) tech-
 25 niques, such as parallel computing, by allowing to deal better with a large
 26 number of categories. Finally, we can find the implementation of the more
 27 recent advances in simulation of lithological data. In the next section we
 28 briefly recall the methodological framework. In Section 3 we illustrate the
 29 main features of spMC by examining a case study (Section 4). Concluding
 30 remarks are addressed in Section 5.

31 **2. Background on spatial Markov chain in geostatistics**

32 The spMC package provides several functions to deal with categorical
 33 spatial data and continuous lag Markov chain, where the lag is the difference
 34 between two spatial positions. Traditionally, a Markov chain is described
 35 by a probabilistic temporal model for one-dimensional discrete lags, i.e. the
 36 model quantifies the probability to observe any specific state in the future
 37 given the knowledge of the current state. The extension of this concept arises
 38 by the definition of a Markov process involving continuous multidimensional
 39 lags in a d dimensional space.

40 We consider the stationary transition probability between two states (or
 41 categories), i and j , in two locations, \mathbf{s} and $\mathbf{s} + \mathbf{h}$, namely

$$t_{ij}(\mathbf{h}) = \Pr(Z(\mathbf{s} + \mathbf{h}) = j | Z(\mathbf{s}) = i), \forall i, j = 1, \dots, K,$$

42 where K is the total number of states that the random variable Z can assume
 43 as outcome and \mathbf{h} is a multidimensional lag of dimension. In continuous-lag

44 formulation of a Markov chain model (Carle and Fogg, 1997) the transition
 45 probability $t_{ij}(\mathbf{h})$ is the element in the i -th row and in the j -th column of
 46 the matrix $\mathbf{T}(\mathbf{h})$ such that

$$\mathbf{T}(\mathbf{h}) = \exp(\|\mathbf{h}\|\mathbf{R}_{\mathbf{h}}). \quad (1)$$

47 The transition rate matrix $\mathbf{R}_{\mathbf{h}}$ depends on the direction given by the lag \mathbf{h} .

48 Carle and Fogg (1997) introduced an approximation of the rate matrix
 49 $\mathbf{R}_{\mathbf{h}}$ by the ellipsoidal interpolation which makes the rate matrix for the di-
 50 rection of \mathbf{h} dependent on the rate matrices $\mathbf{R}_{\mathbf{e}_k}$ estimated for the main axial
 51 directions. The vector \mathbf{e}_k indicates the standard basis vector of dimension
 52 d , whose k -th component is one and the others are zero. In particular, the
 53 matrix $\mathbf{R}_{\mathbf{e}_k}$ can be computed as

$$\mathbf{R}_{\mathbf{e}_k} = \text{diag}(\boldsymbol{\ell}_{\mathbf{e}_k})^{-1} [\mathbf{F}_{\mathbf{e}_k} - \mathbf{I}],$$

54 or for the reversibility of the chain as

$$\mathbf{R}_{-\mathbf{e}_k} = \text{diag}(\mathbf{p}) \mathbf{R}_{\mathbf{e}_k}^{\top} \text{diag}(\mathbf{p})^{-1},$$

55 where $\boldsymbol{\ell}_{\mathbf{e}_k}$ is the mean vector of the stratum thicknesses/lengths along the di-
 56 rection \mathbf{e}_k , the matrix $\mathbf{F}_{\mathbf{e}_k}$ denotes the transition probabilities for consecutive
 57 blocks made of adjacent points with the same category, \mathbf{I} is the identity ma-
 58 trix, and \mathbf{p} is the vector of relative frequencies corresponding to the estimate
 59 of the stationary distribution.

60 The rate $r_{ij,\mathbf{h}}$ in the i -th row and j -th column of the matrix $\mathbf{R}_{\mathbf{h}}$ is then
 61 calculated as

$$|r_{ij,\mathbf{h}}| = \sqrt{\sum_{k=1}^d \left(\frac{h_k}{\|\mathbf{h}\|} r_{ij,\mathbf{e}_k} \right)^2}, \quad (2)$$

62 where $r_{ij,\mathbf{h}}$ is non-positive when $i = j$, otherwise it is non-negative; d rep-
 63 resents the dimension of the lag \mathbf{h} (and hence the number of coordinates of
 64 \mathbf{s}), and r_{ij,\mathbf{e}_k} denotes the components in the i -th row and j -th column of the
 65 matrix $\mathbf{R}_{\mathbf{e}_k}$.

66 From a statistical viewpoint, two problems arise. The former is related
 67 to how to estimate the components $r_{ij,\mathbf{h}}$, while the latter is associated to the
 68 formulation of the conditional probability used for simulations and predic-
 69 tions.

70 spMC provides a variety of estimation methods. We implemented the
 71 mean length method and the maximum entropy method suggested in Carle
 72 and Fogg (1997) and Carle (1999). These methods are both based on the
 73 mean lengths \bar{L}_{i,\mathbf{e}_k} and the transition probabilities of embedded occurrences
 74 f_{ij,\mathbf{e}_k}^* , which are the components of the matrix $\mathbf{F}_{\mathbf{e}_k}$. The autotransition rates
 75 are derived by $r_{ii,\mathbf{e}_k} = -1/\bar{L}_{i,\mathbf{e}_k}$, while the other rates are calculated as $r_{ij,\mathbf{e}_k} =$
 76 $f_{ij,\mathbf{e}_k}^*/\bar{L}_{i,\mathbf{e}_k}$, i.e. for any $i \neq j$. The mean lengths are usually computed by
 77 means of the average of the observed stratum thicknesses/lengths, while the
 78 transition probabilities of embedded occurrences are estimated as the average
 79 of the relative transition frequencies, or through an iterative procedure based
 80 on the entropy (Goodman, 1968).

81 A maximum likelihood method is implemented in which we consider
 82 the stratum thicknesses/lengths distributed as log-normal random variables
 83 (Ritzi, 2000). There also exist robust alternatives for estimating the mean
 84 lengths which are based on the trimmed median and the trimmed average.

Finally, we have considered a least squares approach in which we mini-
 mize the sum of the squared discrepancies between the empirical transition

probabilities and theoretical probabilities given by the model (1). Such minimization is performed under the constraints (Carle and Fogg, 1997):

$$\begin{aligned} \sum_{j=1}^K r_{ij,\mathbf{h}} &= 0, \quad \forall i = 1, \dots, K \text{ and} \\ \sum_{i=1}^K p_i r_{ij,\mathbf{h}} &= 0, \quad \forall j = 1, \dots, K, \end{aligned}$$

85 where p_i denotes the i -th component of the vector \mathbf{p} .

86 In order to perform lithological simulations and predictions, an approxi-
87 mation of the following conditional probability must be considered:

$$\Pr \left(Z(\mathbf{s}_0) = j \mid \bigcap_{l=1}^n Z(\mathbf{s}_l) = z(\mathbf{s}_l) \right), \quad \forall j = 1, \dots, K, \quad (3)$$

88 where \mathbf{s}_0 denotes a simulation or prediction location, \mathbf{s}_l represents the l -th
89 spatial position which corresponds to the l -th observation, and $z(\mathbf{s}_l)$ indi-
90 cates the observed value of the random variable $Z(\mathbf{s}_l)$. The approximation
91 proposed by Carle and Fogg (1996) is based on indicator Kriging and CoK-
92 riging methods, which are then adjusted by a quenching procedure based on
93 the simulated annealing method. Other approximations are based on path
94 methods (Li, 2007; Li and Zhang, 2007), while those that are based on the
95 Bayesian entropy perspective (Christakos, 1990) were considered by Bogaert
96 (2002) and modified by Allard et al. (2011).

97 The Kriging approximations are calculated through a linear combination
98 of weights, i.e.

$$\Pr \left(Z(\mathbf{s}_0) = j \mid \bigcap_{l=1}^n Z(\mathbf{s}_l) = z(\mathbf{s}_l) \right) \approx \sum_{l=1}^n \sum_{i=1}^K w_{ij,l} c_{il},$$

99 where

$$c_{il} = \begin{cases} 1 & \text{if } z(\mathbf{s}_l) = i, \\ 0 & \text{otherwise,} \end{cases}$$

100 and the weight $w_{i,j,l}$ is the component in the i -th row and j -th column of the
 101 matrix \mathbf{W}_l ; such weights are calculated by solving the following system of
 102 linear equations:

$$\begin{bmatrix} \mathbf{T}(\mathbf{s}_1 - \mathbf{s}_1) & \cdots & \mathbf{T}(\mathbf{s}_n - \mathbf{s}_1) \\ \vdots & \ddots & \vdots \\ \mathbf{T}(\mathbf{s}_1 - \mathbf{s}_n) & \cdots & \mathbf{T}(\mathbf{s}_n - \mathbf{s}_n) \end{bmatrix} \begin{bmatrix} \mathbf{W}_1 \\ \vdots \\ \mathbf{W}_n \end{bmatrix} = \begin{bmatrix} \mathbf{T}(\mathbf{s}_0 - \mathbf{s}_1) \\ \vdots \\ \mathbf{T}(\mathbf{s}_0 - \mathbf{s}_n) \end{bmatrix}.$$

103 This system of equations, which can also lead to the CoKriging equations,
 104 is singular. However, it can be solved through the constraints proposed by
 105 Carle and Fogg (1996).

In order to obviate axiomatic problems arising from the Kriging approx-
 imation, the path methods (Li, 2007; Li and Zhang, 2007) considered the
 following approximation under the assumption of conditional independence:

$$\Pr \left(Z(\mathbf{s}_0) = z_i \mid \bigcap_{l=1}^n Z(\mathbf{s}_l) = z(\mathbf{s}_l) \right) \approx \Pr \left(Z(\mathbf{s}_0) = z_i \mid \bigcap_{l=1}^m Z(\mathbf{s}_l) = z_{k_l} \right) \propto \\ \propto t_{k_1 i}(\mathbf{s}_0 - \mathbf{s}_1) \prod_{l=2}^m t_{i k_l}(\mathbf{s}_0 - \mathbf{s}_l).$$

106 These methods are characterized by following a fixed or random path of
 107 unknown points, which are predicted or simulated by conditioning on the of
 108 the previous prediction point.

109 Other approximations were proposed in order to improve the Kriging
 110 deficiencies. In particular, Bogaert (2002) introduced a Bayesian procedure

111 exploiting the maximum entropy, which was successively considered by Allard
 112 et al. (2011) to justify the usage of the following approximation:

$$\Pr \left(Z(\mathbf{s}_0) = z_i \mid \bigcap_{l=1}^n Z(\mathbf{s}_l) = z(\mathbf{s}_l) \right) \approx \frac{p_i \prod_{l=1}^n t_{ik_l}(\mathbf{s}_0 - \mathbf{s}_l)}{\sum_{i=1}^K p_i \prod_{l=1}^n t_{ik_l}(\mathbf{s}_0 - \mathbf{s}_l)}.$$

113 3. spMC features

114 The spMC package is basically a collection of functions not implemented
 115 in other software, which can be grouped according to their purposes as sum-
 116 marized in Table 1. Since the package was designed for intensive geostatis-
 117 tical computations, part of the code deals with parallel computing via the
 118 OpenMP constructs (OpenMP Architecture Review Board, 2008). For ex-
 119 ample, the `setCores()` function permits the user to choose the number of
 120 CPU cores that will be used by the other functions of the spMC package.

121 Some of the functions implement descriptive geostatistical tools, which
 122 are useful for a better understanding of the process and essential for the
 123 parameter estimation of the model.

124 Graphical tools were developed to help the user to choose the model.
 125 These tools are often used for initial evaluations on the input data. From a
 126 visual inspection of these graphics, it is possible to analyze the distribution
 127 of the stratum thicknesses/lengths along a given direction.

128 Once the transition rates have been estimated with the chosen model
 129 fitting algorithm, it is possible to calculate the theoretical transition prob-
 130 abilities for a set of multidimensional lags. This transition probabilities are

Table 1: Most important user functions in the spMC package.

Tasks and functions	Techniques implemented in the spMC package
<i>Descriptive geostatistical tools</i>	
<code>which_lines</code>	Points classification through directional lines
<code>getlen</code>	Estimation of stratum lengths for embedded chains
<code>density.lengths</code>	Empirical densities of stratum lengths
<code>mten</code>	Mean length estimation for embedded chains
<i>Estimations of continuous lag models</i>	
<code>transiogram</code>	Empirical transition probabilities estimation
<code>pemt</code>	Multi-directional transiograms estimation
<code>embed_MC</code>	Transition probabilities estimation for embedded chains
<code>tpfit</code>	One-dimensional model parameters estimation
<code>multi_tpfit</code>	Multidimensional model parameters estimation
<i>Categorical spatial random field simulation and prediction</i>	
<code>sim</code>	Random field simulations and predictions
<code>quench</code>	Quenching algorithm for simulation adjustments
<i>Graphical tools</i>	
<code>plot.transiogram</code>	Plot one-dimensional transiograms
<code>mixplot</code>	Plot multiple one-dimensional transiograms
<code>contour.pemt</code>	Display contours with multi-directional transiograms
<code>image.pemt</code>	Images with multi-directional transiograms
<code>image.multi_tpfit</code>	Images with multidimensional transiograms
<code>boxplot.lengths</code>	Boxplot of stratum lengths
<code>hist.lengths</code>	Histograms of stratum lengths
<i>High performance computational tools</i>	
<code>setCores</code>	Set the number of CPU cores for HPC

131 used in spMC package for simulation of the lithological categories, while
132 predictions are by-products of the function `sim()`.

133 *3.1. Descriptive tools*

134 Most of the descriptive tools of the spMC package are based on graphical
135 analyses, with a subset adopted for inferential purposes. In fact, the study
136 of stratum thicknesses/lengths is relevant for guiding the decision of which
137 computational method to adopt for estimating the mean lengths. The anal-
138 ysis of the empirical distribution of stratum lengths is mainly based on the
139 evaluation of quartiles and extreme values through the basic technique of the
140 boxplot diagrams, which is implemented in the function `boxplot.lengths()`.
141 Another technique is available for the empirical estimation of the stratum
142 lengths distribution, which is performed by the function `density.lengths()`,
143 and it is based on the kernel-smoothing approach.

144 Further descriptive tools are the analyses of empirical, multi-directional
145 and theoretical transiograms. However, the descriptive analysis of the tran-
146 siograms can be performed only after an accurate inferential analysis. For ex-
147 ample, the function `mixplot()` is used to check for probabilistic anisotropies
148 by comparing one-dimensional empirical transiograms along several direc-
149 tion. Similar analyses can be performed also for multidimensional models,
150 e.g. when the function `contour.pemt()` is applied to an object resulting from
151 the function `pemt()`.

152 *3.2. Inferential tools*

153 The implementation of the one-dimensional experimental transiogram
154 computation is based on two subsequent steps. In primis, a selection of points

155 which belong to specific directional-lines is common to all transiogram esti-
156 mation methods. This technique is implemented in the function `which_lines()`,
157 which classifies observation coordinates along a chosen direction. After this,
158 the estimation of the empirical transiogram is performed by counting the
159 transitions among categories along the classified lines. The absolute transi-
160 tion frequencies are then normalized to obtain the transition probabilities as
161 relative frequencies. Both directional classification and transition probabil-
162 ity estimation are performed by the usage of the function `transiogram()`,
163 which also computes the standard errors by assuming the asymptotic nor-
164 mality of the estimates. These standard errors are then used by the function
165 `plot.transiogram()` to produce confidence intervals by the inversion of the
166 Wald type interval for the log odds (Stone, 1996; Brown et al., 2001).

167 One-dimensional theoretical transiograms are computed differently, be-
168 cause they require the estimation of the model parameters for computing
169 the transition probabilities. In practice, the function `tpfit()` allows the
170 selection from three different rate estimation techniques through a specific
171 argument:

- 172 • the mean lengths method (`method = "ml"`), which is based on the esti-
173 mation of mean lengths and the transition probabilities of the embed-
174 ded Markov chains by the functions `m1en()` and `embed_MC()` respec-
175 tively. The resulting quantities are used to estimate the parameters;
- 176 • the maximum entropy algorithm (`method = "me"`), which is iterative
177 and requires few iterations to converge;
- 178 • the iterated least squares technique (`method = "ils"`), which was de-

179 developed for reducing the discrepancies between the experimental tran-
180 siogram and the theoretical model by relaxing the mathematical con-
181 straints on the parameters.

182 Multidimensional transiogram estimation can be viewed as an extention
183 of the one-dimensional methods. The function `multi_tpfite()` allows for
184 the parameter estimation along multiple orthogonal axes. These parameters
185 will be ellipsoidally interpolated for the calculation of transition rates along
186 non-orthogonal directions. As for the one-dimensional models, the three
187 estimation techniques previously exposed are chosen by a specific argument
188 of the functions `multi_tpfite()`.

189 Multi-directional transiograms are computed either with ellipsoidal inter-
190 polation or without. The function `pent()` allows for the computation of the-
191 oretical transition probabilities for any chosen direction without ellipsoidal
192 interpolation.

193 *3.3. Simulations and predictions tools*

194 Three different techniques were considered to approximate the conditional
195 probability in (3). The function `sim()` allows the selection of the method for
196 simulation, in particular:

- 197 • the Kriging methods are implemented for the indicator Kriging and
198 indicator CoKriging. The Kriging approach is usually adopted for pre-
199 diction, but it is used in the `spMC` package mainly for sequential simula-
200 tions. In addition, it is possible to adjust the simulations by performing
201 the quenching algorithm implemented in the function `quench()`;

- 202 • a fixed and random path algorithms are available, and they can be se-
203 lected by logical argument `fixed`. By default a random path algorithm
204 is performed, because its results are more consistent with reality;
- 205 • the maximum entropy approach, which was proposed by Allard et al.
206 (2011) for avoiding the entropy optimization. It performs an aggre-
207 gation of transition probabilities to approximate the optimal solution.
208 This particular setting reduces the computations with respect to the
209 Bogaert's proposal (2002).

210 Furthermore, these three methods produce also predictions by combining
211 the transition probabilities calculated through the theoretical model in (1),
212 where the transition rates in the matrix \mathbf{R}_h are calculated as in (2). In
213 doing so, a considerable computational efficiency is achieved for computing
214 an approximation of the distribution at each point in the simulation grid.

215 4. Case study

216 The package includes the 3D data-set ACM, related to a sediment deposit
217 of about 300 m in longitude (X direction), 500 m in latitude (Y direction)
218 and 400 m in depth (Z direction), located in Scorzé area (Venetian plain, NE
219 Italy) (Figure 1), consisting of a collection of eleven simplified lithostratigraf-
220 ical borehole data. The lithologies of these boreholes were simplified in three
221 different cases. In the first categorical data set (MAT5) the local lithology
222 was simplified in five lithologies (Clay, Sand, Mix of Sand and Clay, Gravel,
223 Mix Sand and Gravel), in the second one (MAT3) in three lithologies (Clay,
224 Sand, Gravel) and finally the third one the lithostratigraphy was simplified

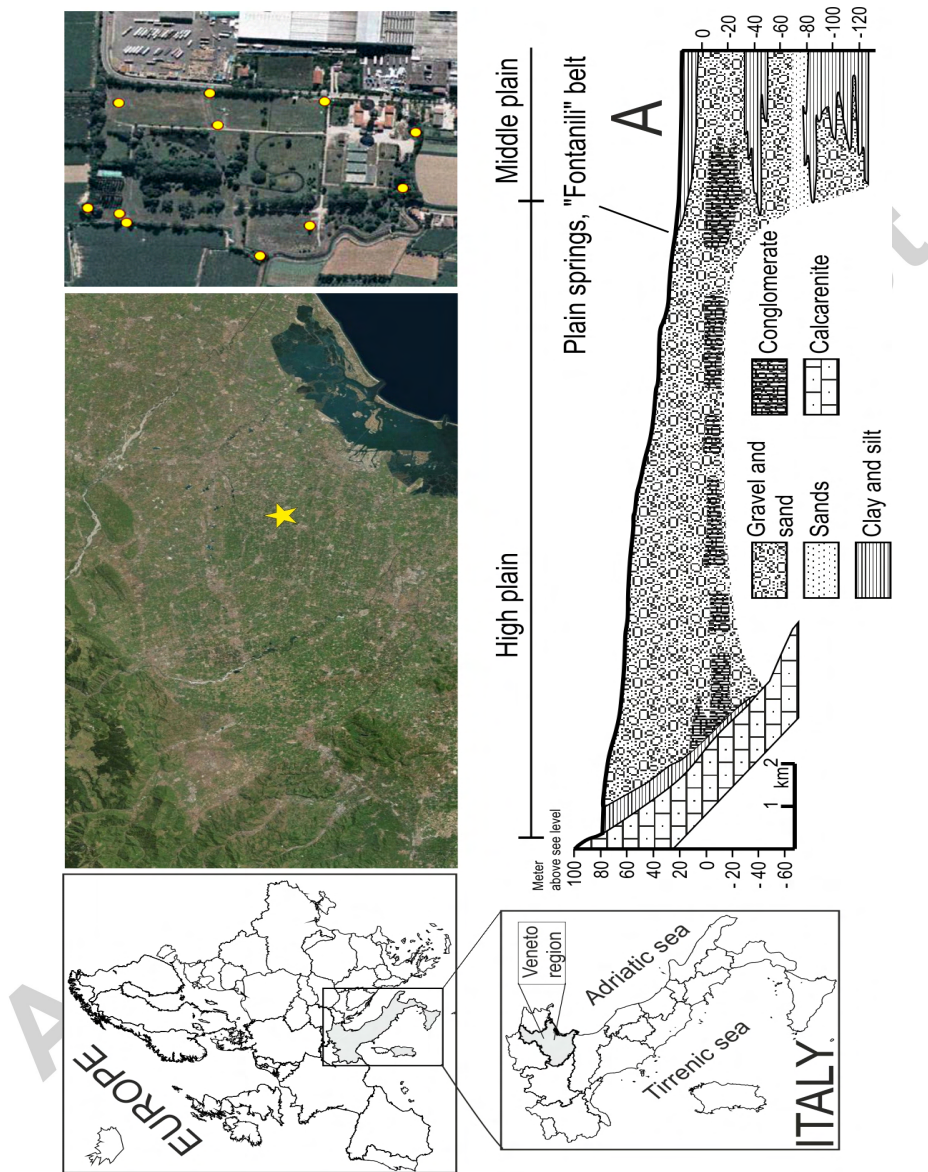


Figure 1: Geographical location of the borehole data.

225 in only two permeability categories (TRUE, FALSE). Geologically Venetian
226 plain can be roughly divided in “high”, “low” plain. The high plain is es-
227 sentially of fluvial origin, but also glacial and fluvioglacial origin near the
228 pre-Alps. This area is principally composed of gravel, particularly the sedi-
229 ments are made by very permeable gravel and pebbly materials. Transition
230 between the high and low plain, of about 2-5 kilometers wide, is represented
231 by the “fontanili” belt. In this zone the gravels decrease in thickness split-
232 ting them into sub-horizontal gravelly layers separated by silty and/or clayey
233 beds, sometimes interbedded with clay layers. The low plain starts where
234 the gravel layers move to sand until the Adriatic coast. Low plain presents
235 a subsoil composed essentially by silt and clay layers interposed with sandy
236 layers. In this part the gravels are absent, with some exceptions found, at
237 considerable depths (e.g. up to 300 meters in depth)(Carraro et al., 2013;
238 Fabbri et al., 2011). In the high plain an undifferentiated aquifer is present,
239 where water table is at maximum depth, this aquifer Southeastern becomes
240 a multi-layered confined or semi-confined aquifer system directly connected
241 with the unconfined. The water table outcrops in the most depressed zones
242 originating the typical plain springs called “fontanili”, where the water table,
243 being very shallow, intersects the topographic surface (Vorlicek et al., 2004;
244 Fabbri and Piccinini, 2013). This discharge band of the unconfined aquifer
245 can be from 2 to 10 kilometers wide, draining the unconfined aquifer and
246 representing the source of some important Venetian river. Hydrogeologically
247 ACM data set concerns the area southern of the “fontanili” belt in area of
248 essentially gravelly multi-layered confined or semi-confined aquifer system.

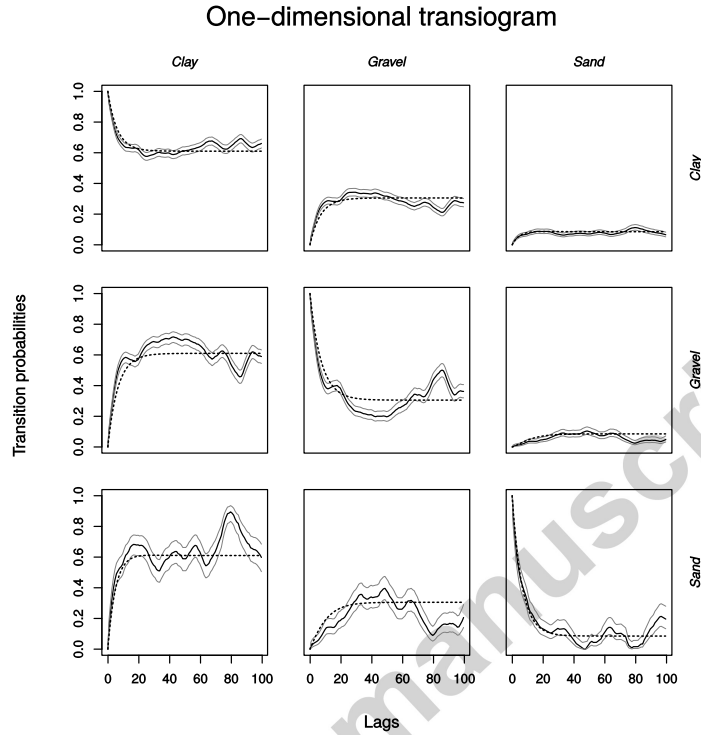


Figure 2: Empirical (full black line) and theoretical (dashed line) transiogram along Z direction. They are calculated with the MAT3 variable. The light-grey lines correspond to the upper and lower confidence bounds for 99% coverage probability.

249 4.1. One-dimensional lags model

250 The empirical transiogram exposed in Figure 2 is computed with 100
 251 lags of 1 meter by considering all couples of points along Z direction within
 252 a maximum distance of 100 meters. The light-grey lines corresponds to the
 253 upper and lower confidence bounds calculated with 99% coverage probability.
 254 From a graphical inspection of the transiogram, it is possible to establish if
 255 the process is stationary. In fact, the empirical transition probabilities should
 256 approximately converge to the relative frequency of the observed materials

257 as the lag-length tends to infinity (see theoretical transiogram by looking at
258 each column in Figure 2). For this reason, the transition probabilities (by
259 columns) corresponding to the farthest distances are respectively close to
260 0.62, 0.30 and 0.08 for Clay, Gravel and Sand.

261 By comparing two or more transiograms drawn for different directions,
262 one can check if there is directional dependence on the data (especially if
263 these are located on a regular sample grid). The process is anisotropic if
264 the transition probabilities are dependent on the directions. In most cases,
265 this aspect is more obvious when the distances between points along different
266 directions are measured at different scales. For example, the distance between
267 points along Z direction can be measured in meters, while it is expressed in
268 kilometers along X and/or Y direction. However, a more quantitative method
269 for inspecting this issue makes use of multidirectional transiograms and is
270 useful when relatively abundant data are available in all three dimensions.

271 Multidirectional transiograms are based on theoretical transition proba-
272 bilities calculated from the estimates of transition rates per multiple chosen
273 directions. This method exploits the implementation of the `tpfit_ml()` func-
274 tion, which is computationally faster than the `tpfit_me()` function. Once the
275 transition probabilities are calculated for specific lags, they can be organized
276 and represented on few graphics as in the left column of Figure 3.

277 *4.2. Multidimensional lags model*

278 Multidimensional models are required to calculate transition probabilities
279 in multidimensional spaces. In fact, even if it is possible to estimate for any
280 direction the transition rates, and hence the corresponding probabilities, it
281 is not computationally feasible to deal with one-dimensional models along

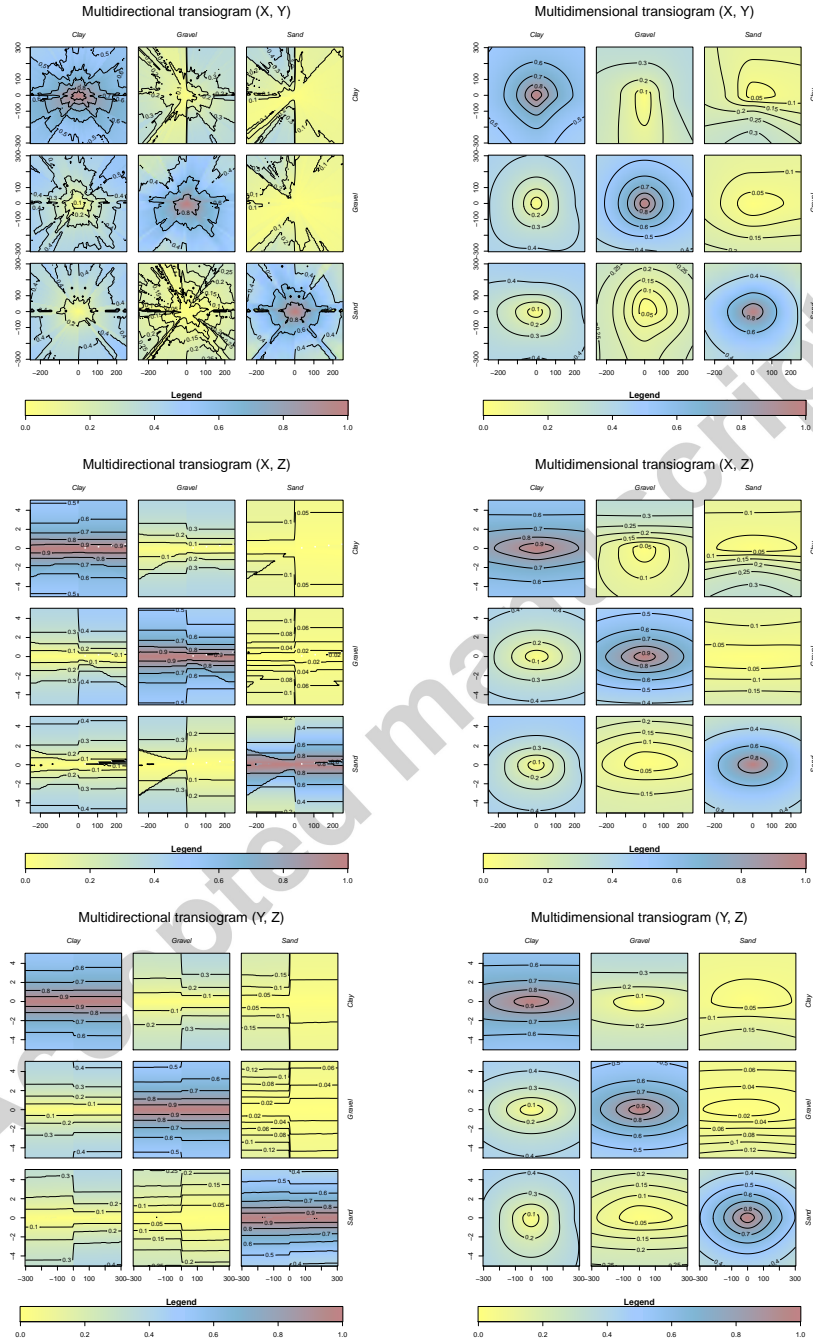


Figure 3: Multidirectional transiograms, and multidimensional transiograms derived from the interpolation of the theoretical model in (1).

282 multiple directions. Multidimensional model interpolate the transition rates
283 along the main axis to obtain a suitable approximation. In so doing, the
284 resulting transition probabilities are more regular, as shown in Figure 3.
285 Since the evaluation of these probabilities is computationally more efficient,
286 it is preferable to adopt theoretical probabilities calculated with interpolated
287 rates, especially when the number of points in the simulation grid is large.

288 The transition probabilities shown in the right column of graphics in Fig-
289 ure 3 share some common patterns with those exposed on the left column.
290 This tool is used to study the probabilistic anisotropy along several direc-
291 tions, the juxtaposition of categories, and the variations of the transition
292 probabilities with respect to both the direction and the distance from the
293 center of each representation.

294 *4.3. Spatial simulations and predictions*

295 From a geological viewpoint, spatial simulations and predictions are nec-
296 essary tools for lithological reconstruction and mapping. However, these
297 statistical techniques can be computationally intensive, and therefore, ex-
298 ploitation of HPC techniques can be advantageous.

299 The main computational issues in classical geostatistics are related to the
300 inversion of a variance-covariance matrix to obtain Kriging predictions for a
301 large number of points in the simulation grid. In this context, both indicator
302 Kriging and CoKriging must solve a system of simultaneous equations where
303 the only few k -nearest neighbors are used instead of the whole observations.
304 Similarly, the method proposed by Allard et al. (2011) can also use a reduced
305 conditional probability for better computational achievements (even when
306 parallel computing is not performed). In the following, a value of $k = 12$ was

307 considered, which is the default value of the function `sim()`. The choice of
 308 k is subjective, because, at the best of our knowledge, no selection methods
 309 for k have been developed for lithological data yet.

310 To show the computational advantages of the implemented algorithms, a
 311 regular simulation grid is constructed within the sample space. It consists
 312 in $21 \times 21 \times 21$ simulation points, which cover a volume of $293\text{m} \times 477\text{m} \times$
 313 400m . Spatial simulations and predictions were performed with a 16-core
 314 AMD64 CPU at 2.4 GHz. Simulations were repeated by using 1, 8 and
 315 16-cores. In particular, Kriging algorithms were executed by considering 32-
 316 nearest neighbors and path algorithms with a search radius of 200 meters.
 317 The efficient maximum entropy method was performed by considering the
 318 transition probabilities among all points (as in the original formulation) and
 319 also with 32-nearest neighbors.

Table 2: Execution time in seconds.

	IK	ICK	FP	RP	MCS	MCSKNN
Serial (1 core)	7.301	7.963	12.554	13.216	97.882	3.886
Parallel (8 cores)	2.738	3.352	12.553	13.212	21.307	1.408
Parallel (16 cores)	2.445	3.233	12.557	13.216	16.948	0.967

320 From Table 2, which reports the elapsed execution time for each algo-
 321 rithm, one can perceive a drastic time reduction with respect to sequential
 322 computing. Indicator Kriging (IK) and CoKriging (ICK) are similar, even if
 323 indicator Kriging performs faster because it processes less information than
 324 CoKriging. Path algorithms are sequential. They are not affected by the
 325 use of multiple processors. However, the fixed path algorithm (FP) perform

326 faster than the random path algorithm (RP), because the sequence of points
 327 to predict is already known and it does not require extra calculations. The
 328 efficient maximum entropy categorical simulations (MCS) are the slowest,
 329 while they become the fastest when the conditional probability is calculated
 330 with the k -nearest neighbors (MCSKNN).

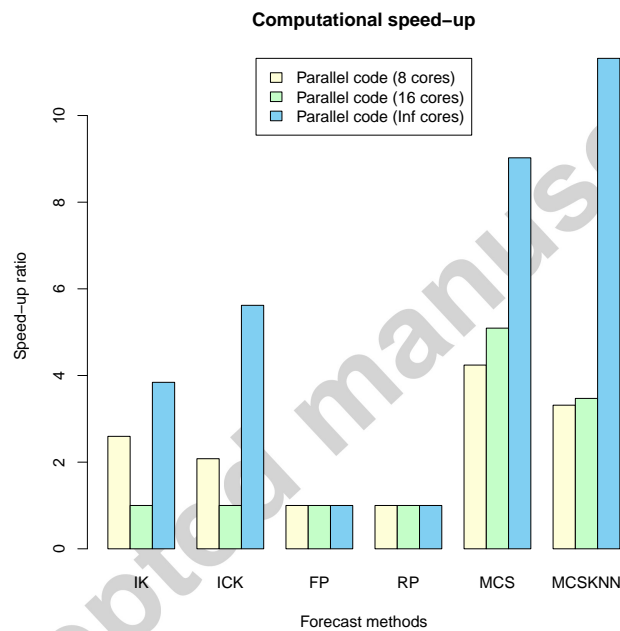


Figure 4: Computational efficiency of the simulation and prediction methods.

331 After looking at the Figure 4, it is possible to establish which algorithm
 332 has a strong impact on high performance computing and scalability (Ku-
 333 mar and Gupta, 1994). In fact, the computational efficiency (measured as
 334 speed-up time) is calculated through the ratio of the execution time between
 335 serial code and parallel. The maximum speed-up with infinity cores can be
 336 approximately computed as the product of the sequential execution time and

337 the fraction of code which is not parallelizable. Figure 4 shows that Kriging
338 methods improve their efficiency when HPC techniques are used. However,
339 the most substantial improvements obtained by parallel computations are
340 shown for the efficient maximum entropy methods.

341 5. Conclusions

342 In comparison with other software used for predicting and simulating
343 lithological categories, spMC is based on a theoretical framework which fo-
344 cuses on transition probabilities rather than covariances/variograms or multi-
345 point geostatistics. The spMC package is able to produce results more effi-
346 ciently by high performance computational techniques, and it can be used on
347 several platforms (Linux, Windows and Mac). It is the unique open-source
348 software which implements several estimation procedures of transition prob-
349 abilities, and the more advanced simulation-prediction techniques based on
350 maximum entropy by geostatistical transition probabilities. Currently, the
351 Gslib library (Deutsch and Journel, 1998) and SGeMS (Remy et al., 2009) are
352 the most known free-source softwares for lithological simulation/prediction
353 based on variogram via Kriging/CoKriging. T-PROGS (Carle, 1999) is based
354 on transition probabilities and Kriging/CoKriging, which is also available as
355 a stand-alone or as an add-on in GMS groundwater model. Mainly, spMC
356 supports parallel computing, and hence its results are produced more ef-
357 ficiently and several lithological categories can be more readily supported.
358 The results of spMC package can be visualized into R through other pack-
359 ages, or exported from R and used in other software. For example, they can
360 be exported in ASC format and imported in GIS software or can be used in

361 groundwater modeling. They can be exported in CSV format and used to
 362 draw probabilistic maps in open-source software like ParaView (Squillacote,
 363 2007) or for the visualization per each category of the occupancy volumes
 364 (see, for example, the probability map of Figure 5 for Sand category).

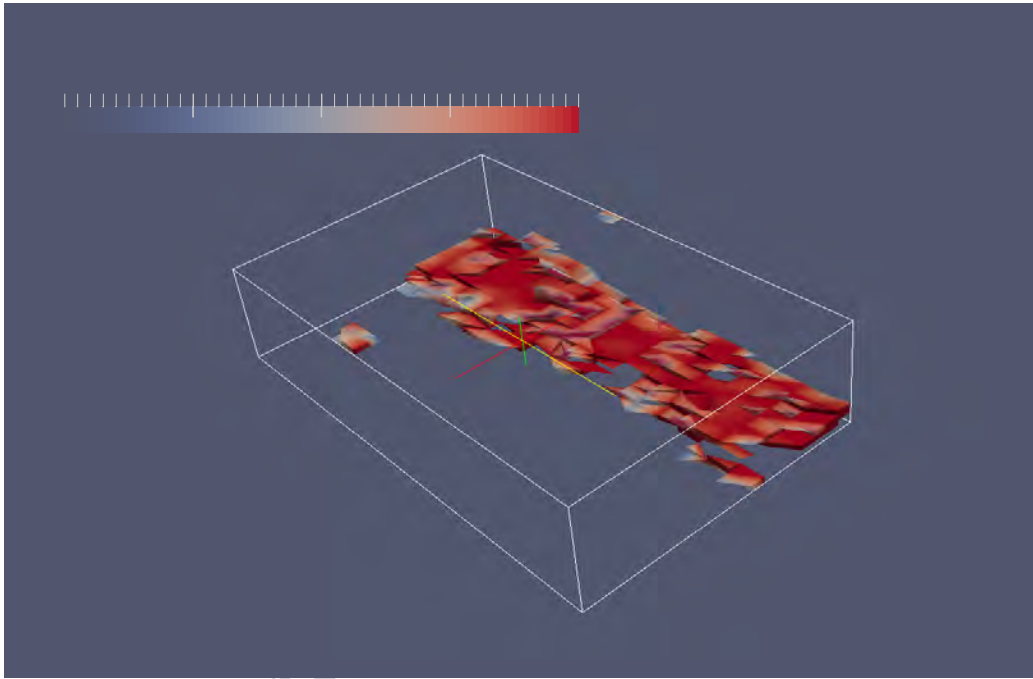


Figure 5: Random-path results, obtained for Sand category, as displayed by Paraview software.

365 The development of the spMC package will continue. In the future, we
 366 plan to include non-parametric estimates of transiograms by means of kernel
 367 methods (Allard et al., 2011) and other probabilistic aggregations (Allard
 368 et al., 2012). Additional validation functions will be also included to allow for
 369 the comparison of simulation/prediction probabilities and actual categorical
 370 variables.

371 **Acknowledgements**

372 Critical reading of the manuscript and comments by professor Graham
373 E. Fogg and one anonymous reviewer are gratefully acknowledged. The au-
374 thors would also like to thank Kelly Toppin for proof-reading the article.
375 This research was supported by grant “GEO-RISKS – Geological, morpho-
376 logical and hydrological processes: monitoring, modeling and impact in the
377 Northeastern Italy” funded by the University of Padua (Italy).

378 **References**

- 379 Allard, D., Communian, A., Renard, P., 2012. Probability aggregation meth-
380 ods in geoscience. *Mathematical Geosciences* 44, 545–581.
- 381 Allard, D., D’Or, D., Froidevaux, R., 2011. An efficient maximum entropy
382 approach for categorical variable prediction. *European Journal of Soil*
383 *Science* 62, 381–393.
- 384 Aquaveo, L.L.C., 2015. Groundwater Modeling System Version 10.1, build
385 date, December 14, 2015. UT, USA.
- 386 Bogaert, P., 2002. Spatial prediction of categorical variables: the Bayesian
387 maximum entropy approach. *Stochastic Environmental Research and Risk*
388 *Assessment* 16, 425–448.
- 389 Brown, L.D., Cai, T.T., DasGupta, A., 2001. Interval estimation for a bino-
390 mial proportion. *Statistical Science* 16, 101–133.
- 391 Carle, S.F., 1999. T-PROGS: Transition probability geostatistical software.

- 392 Carle, S.F., Fogg, G.E., 1996. Transition probability-based indicator geo-
393 statistics. *Mathematical Geology* 28, 453–476.
- 394 Carle, S.F., Fogg, G.E., 1997. Modeling spatial variability with one and
395 multidimensional continuous-lag Markov chains. *Mathematical Geology*
396 29, 891–918.
- 397 Carle, S.F., Labolle, E.M., Weissmann, G.S., Van Brocklin, D., Fogg, G.E.,
398 1998. Conditional simulation of hydrofacies architecture: a transition prob-
399 ability/Markov approach, in: Fraser, G.S., Davis, J.M. (Eds.), *SEPM Hy-
400 drogeologic Models of Sedimentary Aquifers, Concepts in Hydrogeology
401 and Environmental Geology No. 1*. Tulsa, Oklahoma, pp. 147–170.
- 402 Carraro, A., Fabbri, P., Giaretta, A., Peruzzo, L., Tateo, F., Tellini, F., 2013.
403 Arsenic anomalies in shallow Venetian plain (Northeast Italy) groundwa-
404 ter. *Environmental Earth Sciences* 70, 3067–3084.
- 405 Christakos, G., 1990. A Bayesian/maximum-entropy view to the spatial
406 estimation problem. *Mathematical Geology* 22, 763–777.
- 407 Deutsch, C., Journel, A.G., 1998. *GSLIB. Geostatistical Software Library
408 and User's Guide*. Oxford University Press.
- 409 Fabbri, P., Gaetan, C., Zangheri, P., 2011. Transfer function-noise modelling
410 of an aquifer system in NE Italy. *Hydrological Processes* 25, 194–206.
- 411 Fabbri, P., Piccinini, L., 2013. Assessing transmissivity from specific xapacity
412 in an alluvial aquifer in the middle Venetian plain (NE, Italy). *Water
413 Science & Technology* 67, 2000–2008.

- 414 Goodman, L.A., 1968. The analysis of cross-classified data: independence,
415 quasi-independence, and interaction in contingency table with and without
416 missing entries. *Journal of the American Statistical Association* 63, 1091–
417 1131.
- 418 Kumar, V.P., Gupta, A., 1994. Analyzing scalability of parallel algorithms
419 and architectures. *Journal of Parallel and Distributed Computing* 22, 379–
420 391.
- 421 Li, W., 2007. A fixed-path Markov chain algorithm for conditional simulation
422 of discrete spatial variables. *Mathematical Geology* 39, 159–176.
- 423 Li, W., Zhang, C., 2007. A random-path Markov chain algorithm for simu-
424 lating categorical soil variables from random point samples. *Soil Science*
425 *Society of America Journal* 71, 656–668.
- 426 OpenMP Architecture Review Board, 2008. OpenMP Application Program
427 Interface Version 3.0.
- 428 R Core Team, 2016. R: A Language and Environment for Statistical Com-
429 puting. R Foundation for Statistical Computing. Vienna, Austria. URL:
430 <https://www.R-project.org/>.
- 431 Remy, N., Boucher, A., Wu, J., 2009. Applied geostatistics with SGeMS.
432 Cambridge University Press.
- 433 Ritzi, R.W., 2000. Behavior of indicator variograms and transition probabili-
434 ties in relation to the variance in lengths of hydrofacies. *Water resources*
435 *research* 36, 3375–3381.

- 436 Sartore, L., 2013. spMC: Modelling Spatial Random Fields with Continuous
437 Lag Markov Chains. *R Journal* 5.
- 438 Squillacote, A., 2007. *The ParaView Guide*. Kitware.
- 439 Stone, C.J., 1996. *A course in probability and statistics*. Duxbury Press
440 Belmont.
- 441 Vorlicek, P.A., Antonelli, R., Fabbri, P., Rausch, R., 2004. Quantitative hy-
442 drogeological studies of Treviso alluvial plain (north east of Italy). *Quar-*
443 *terly Journal of Engineering Geology and Hydrogeology* 37, 23–29.
- 444 Weissmann, G.S., Carle, S.F., Fogg, G.E., 1999. Three-dimensional hydrofa-
445 cies modeling based on soil surveys and transition probability geostatistics.
446 *Water Resources Research* 35, 1761–1770.
- 447 Weissmann, G.S., Fogg, G.E., 1999. Multi-scale alluvial fan heterogene-
448 ity modeled with transition probability geostatistics in a sequence strati-
449 graphic framework. *Journal of Hydrology* 226, 48–65.